Theoretical Studies on 2-Hexylthieno[3,2-*b*]thiophene End-Capped Oligomers for Organic Semiconductor Materials[†]

Young Hee Park, Yun-Hi Kim,[‡] Soon-Ki Kwon,[§] In Sun Koo, and Kiyull Yang[*]

Department of Chemistry Education and Research Institute of Natural Science, Gyeongsang National University,
Jinju 660-701, Korea. [*]E-mail: kyang@gnu.ac.kr
[‡]Department of Chemistry and Research Institute of Natural Science, Gyeongsang National University, Jinju 660-701, Korea
[§]School of Materials Science & Engineering and ERI, Gyeongsang National University, Jinju 660-701, Korea
Received December 16, 2011, Accepted January 5, 2012

The reorganization energy and the spectroscopic properties of 2,6-bis(5'-hexyl-thieno[3,2-*b*]thiophene-2'-yl)naphthalene (DH-TNT) and 2,6-bis(5'-hexyl-thieno[3,2-*b*]thiophene-2'-yl)anthracene (DH-TAT), which are composed of an acene unit and alkylated thienothiophene on both sides, as organic materials for display devices were calculated and the results were compared with experimental values. The lower reorganization energy of the DH-TAT over the DH-TNT calculated by the density functional theory is attributed to a smaller vibrational distortion because of the heavier building block of DH-TAT, and it shows a good field effect performance over the DH-TNT. The calculated spectra and the other spectroscopic characteristic of the compounds are well consistent with those of observed results.

Key Words : Reorganization energy, Organic thin film transistor, Hole transport, Organic semiconductor, Density functional theory

Introduction

Conducting organic materials have recently seen much attention with respect to fabrication of electronic devices. These materials show conductivity despite their not being a metal electrically and having no free electrons.

Among organic semiconductor materials, conjugated organic molecules have been increasingly used as active materials for optoelectronic devices such as field-effect transistors (FET's),[1-5] light-emitting diodes (LED's),[6-9] and photovoltaic and solar cells.[10-13] The devices fabricated using organic semiconductors are known as organic devices, and organic thin film transistors (OTFT) are one class of these devices.[14] This transistor is one of the key components for the switching circuitry in flexible display devices.

These materials used in OTFTs offer advantages of easy fabrication, mechanical flexibility and low cost. A number of organic materials including acenes and their derivatives show useful field-effect transistor performance, which can be characterized by their carrier mobility and on/off current ratios. Among the acene-related compounds, pentacene is the most popular molecule as it shows good carrier (hole) mobility up to ~5 cm^2/Vs, exceeding that of amorphous silicon transistors.[15-17]

Recently, many of the organic semiconductors used for the fabrication of the OTFTs have been derived from thiophene-based π-conjugated systems, oligothiophene,[18,19] carbon-sulfur fused rings,[20] acenes,[21,22] phthalocyanines,[23,24] poly-thiophene,[25] and polythienylenevinylenes.[26] In particular, the acene and oligothiophene derivatives represent two of the most heavily studied series of compounds used in organic semiconductors.[27-30]

The field-effect mobility of α,ω-dihexylsexithiophene, one of the most widely investigated materials, reaches 0.1 cm^2/Vs depending on the material used for the gate insulator and the fabrication method.[31,32] Recently, new acene derivatives that are composed of a naphthalene or anthracene core unit and alkylated thienothiophene on both sides was reported.[33] The thienothiophene-naphthalene-thienothiophene moiety or thienothiophene-anthracene-thienothiophene moiety in reported molecules, which are composed of fused aromatics, would be expected to have a suitable HOMO and solid-state structure for use as a *p*-channel TFT semiconductor. In addition, it was reported that the barrier to oxidation could be higher than for pentacene, because the oxygen addition in these molecules occurs across the central ring. In the fused aromatics, the hexyl group is introduced on the α-position of sulfur of thienothiophene for increasing their capacity for self-assembling into close-packed structures.

Furthermore, it was reported that a hybrid acene-thiophene molecule shows good thermal and oxidation stability as well as good TFT characteristics.[34,35] It was also reported that TFT characteristics could be increased by replacing bithio-phene with fused thienothiophene.[36-38]

In this work, the TFT property of a fused aromatic molecule was studied theoretically. The electronic properties and TFT characteristics of 2,6-bis(5'-hexyl-thieno[3,2-*b*]thio-phene-2'-yl)naphthalene (DH-TNT) and 2,6-bis(5'-hexyl-thieno[3,2-*b*]thiophene-2'-yl)anthracene (DH-TAT), which were synthesized by Kwon and coworkers, were calculated

---

[†]This paper is dedicated to the memory of the late Professor Saul Wolfe of the Simon Fraser University, Canada.

DH-TNT

DH-TAT
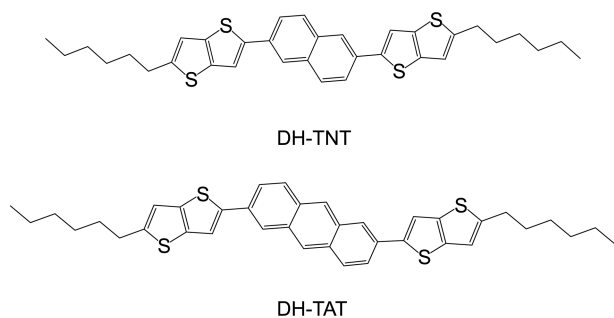
Scheme 1. *p*-type organic semiconductor materials.

and the results were compared with experimental values.[33]

Computational Method

Many theoretical characterizations including the charge transport properties of organic materials for the OTFTs are well described by Brédas *et al.*[39] The work was mainly achieved using the density functional theory (DFT) and showed the reliability of the DFT to reproduce experimental findings. The measured hole and electron mobilities of oligoacene crystals showed a band hopping transition occurring at about room temperature.

Hopping of a hole or electron can be described as an electron transfer (ET) reaction from a charged, relaxed unit to an adjacent neutral unit, and the mobility depends on the electron transfer rate. The hole transport in the *p*-type organic semiconductor materials can be described as a self-exchange reaction (1).

$$M^+ + M \rightarrow M + M^+ \tag{1}$$

Here, M^+ refers to the molecule in the cationic state, and M refers to the adjacent molecule in the neutral state. At high temperatures, the hopping rates for the self-exchange reactions are given in Eq. (2), according to the semi-classical Marcus theory.[40]

$$k_{ET} = \frac{4\pi^2}{h}\frac{1}{\sqrt{4\pi\lambda k_B T}}t^2 \exp\left(-\frac{\lambda}{4k_B T}\right). \tag{2}$$

Here, λ is a reorganization energy that describes the strength of the hole (electron)-vibration coupling energy of a charge localized on a single molecule, and it needs to be small for efficient transport. The electronic coupling term (*t*) between two adjacent molecules, often called transfer integral largely depends upon the orbital overlap between the two, and it needs to be large for higher mobility.[41] The intramolecular reorganization energy is a purely intrinsic property of a single molecule, and the energy consists of two terms corresponding to the structural relaxation energies λ_N and λ_C as illustrated in Figure 1.

The reorganization energies can be estimated in two ways, with an adiabatic process using the adiabatic potential energy surface, shown in Figure 2, and with a normal-mode analysis. In the former procedure, total adiabatic reorganization energy $(\lambda_{tot} = \lambda_N + \lambda_C)$, is a sum of the relaxation or reorganization energies given in Eqs. (3) and (4),[41-45]
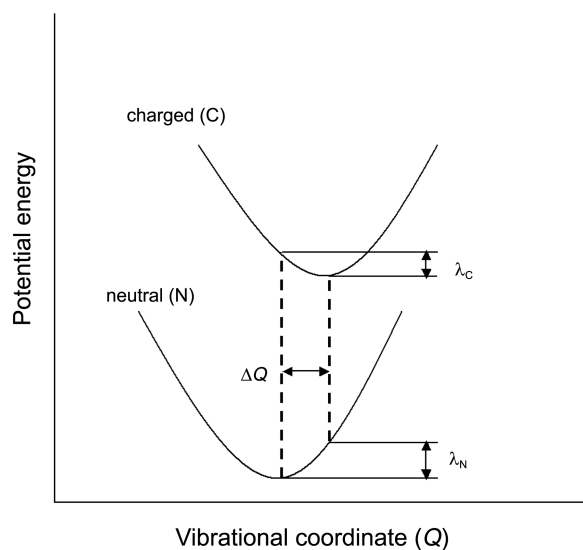

Figure 1. Schematic diagram of general adiabatic energy surfaces corresponding to the ionization process. *Q* is a normal-mode displacement and λ_N and λ_C are relaxation energies described at Eqs. (3) and (4), respectively.

$$\lambda_N = E_N(rel) - E_N \tag{3}$$

$$\lambda_C = E_C(rel) - E_C \tag{4}$$

where $E_N(rel)$ and $E_C(rel)$ are the energies of the neutral state in the optimized (relaxed) geometry of a charged molecule and the energies of a charged state in the optimized geometry of a neutral molecule, respectively. E_N and E_C are the energies of the neutral state in the optimized geometry of a neutral molecule and the energies of the charged state in the optimized geometry of a charged molecule, respectively.

In the latter procedure, the total reorganization energies can be estimated by summing the contributions of each vibrational mode based on a harmonic oscillation approximation:

$$\lambda_{N(C)} = \Sigma \lambda_i = \Sigma \frac{1}{2} k_i \Delta Q_i^2 \tag{5}$$

where ΔQ_i represents the displacement along vibrational coordinate Q_i between the geometries of the two states, and k_i is the corresponding force constant.

All quantum mechanical calculations were performed using the Gaussian 98[46] and Gaussian 03[47] programs and the structures and the adiabatic reorganization energies were evaluated at the DFT of Becke's 3-parameter hybrid method using the correlation functional of Lee, Yang, and Parr (B3LYP)[48] at the 6-31G(d,p) level. Total adiabatic reorganization energies were calculated using Eqs. (3) and (4), and the evaluation of reorganization energies represented by Eq. (5) with normal mode analysis were performed by the DUSHIN program written by Reimers.[44]

The time-dependent density functional theory (TD-DFT)[49] with a B3LYP functional and 6-31G(d,p) basis set was applied to evaluated band gaps and absorption spectra. The ZINDO method[50,51] was also applied to obtain the absorption properties of the compounds for the comparison.
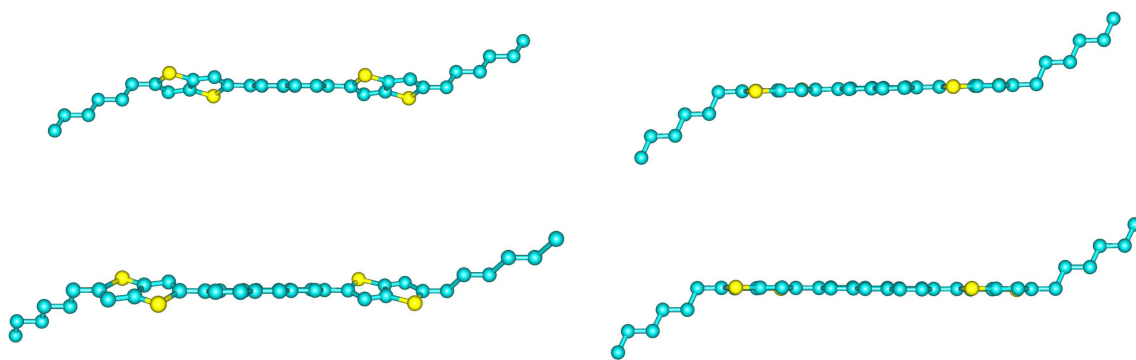
Figure 2. The geometries of neutral (left) and cation (right) for DH-TNT (top) and DH-TAT (bottom). Hydrogen atoms are omitted for clarity.

Geometry optimizations for excited states geometry were performed with the HF/CIS method[52] with a 3-21G(d) basis set. Using the optimized geometries for the excited state geometry, their fluorescence spectra and oscillator strengths were obtained with the TD-DFT method.[53]

Results and Discussion

Geometries of neutral and cationic states for DH-TNT and DH-TAT are shown in Figure 2. The dihedral angle between naphthalene (or anthracene) and hexylthienothiophene decreased from ~27° (or ~28°) at the optimized geometry for the neutral state to ~0° at the optimized geometry for the cation state.

The reorganization energy of DH-TNT and DH-TAT were estimated in two ways: an adiabatic process and a normal-mode analysis. As shown in Table 1, the reorganization energy of DH-TAT was smaller than that of DH-TNT. This supports the experimental results in which the hole mobility and on/off ratio of DH-TAT were higher than those of DH-TNT. This is attributed to DH-TAT having a large fused anthracene unit. A normal mode analysis was also performed to examine the effect of the vibrational mode on the reorganization energy.

The partition of the reorganization energies for the hole transfer in DH-TNT and DH-TAT is given in Tables 2 and 3. Graphical representations of the partition are also shown in

Figure 3.

As the Tables demonstrate, the main contribution of hole transfer to the reorganization energy comes from the vibra-

Table 2. Vibrational frequencies ω (cm^{-1}) and relaxation energies λ (eV) associated with the totally symmetric vibrations of DH-TNT in neutral and their singly oxidized states[a]

DH-TNT					
neutral			cation		
ω	Q	$\lambda_{N,\omega}$	ω	Q	$\lambda_{C,\omega}$
37	-1.485	0.005	16	2.540	0.006
44	-5.698	0.089	26	3.707	0.023
109	-1.552	0.016	85	-0.940	0.005
1476	0.449	0.018	118	-0.916	0.006
1559	0.317	0.010	1188	0.357	0.009
1580	0.314	0.010	1283	0.261	0.005
1675	-0.262	0.007	1359	-0.253	0.005
			1374	0.376	0.012
			1498	0.292	0.008
total		0.217			0.155

[a]The vibrations which correspond to the reorganization energy of 0.005 eV or more are summarized.

Table 3. Vibrational frequencies ω (cm^{-1}) and relaxation energies λ (eV) associated with the totally symmetric vibrations of DH-TAT in neutral and their singly oxidized states[a]

DH-TAT					
neutral			cation		
ω	Q	$\lambda_{N,\omega}$	ω	Q	$\lambda_{C,\omega}$
15	-2.517	0.006	11	-3.338	0.008
36	4.386	0.043	113	-0.818	0.005
41	3.376	0.029	1222	0.311	0.007
101	1.108	0.008	1435	0.230	0.005
1475	0.371	0.013	1569	-0.358	0.012
1553	0.236	0.005			
1580	-0.220	0.005			
1595	-0.302	0.009			
1671	0.258	0.007			
total		0.177			0.118

[a]The vibrations which correspond to the reorganization energy of 0.005 eV or more are summarized.

Table 1. Computed reorganization energies observed hole mobility (μ) and on/off ratio

Molecule	Computational value				Experimental value[c]	
	Method[a]	Reorganization E (eV)			μ^b (cm^2/Vs)	on/off ratio
		λ_N	λ_C	λ_{tot}		
DH-TNT	AP	0.143	0.177	0.320	0.084	8.8×10^5
	NM	0.217	0.155	0.372		
DH-TAT	AP	0.132	0.145	0.277	0.14	6.3×10^6
	NM	0.177	0.118	0.295		

[a]AP and NM refer to the adiabatic potential surfaces method and normal mode method, respectively. [b]Top contact device deposited at T_s = 100 °C (DH-TNT) and T_s = 120 °C (DH-TAT) on 1,1,1,3,3,3-hexamethyldisilazane (HMDS)-treated SiO$_2$. [c]Values from Ref. 33.
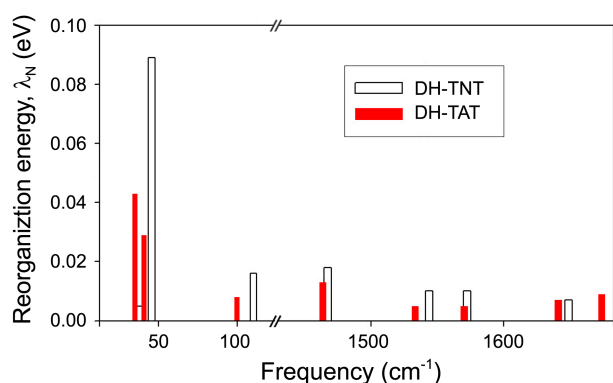
Figure 3. Graphical representation for reorganization energies of DH-TNT and DH-TAT for electron hopping at vibrational frequencies.
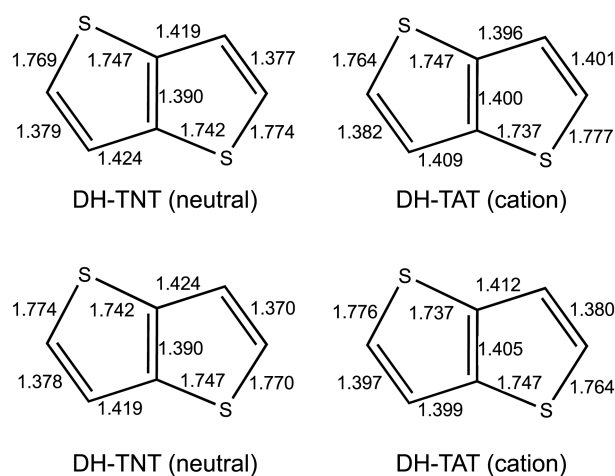

Figure 4. Bond length (Å) of thienothiophene moiety in DH-TNT and DH-TAT.

tions at 44 cm^{-1} (in DH-TNT) or 36 cm^{-1} (in DH-TAT) which make up the torsional mode of vibration along the C-C bond between the thienothiophene and acene moiety of the molecule. The vibrational modes at around 1470-1580 cm^{-1} and over 1580-1675 cm^{-1} correspond to π-bond stretching of thienothiophene and acenes (naphthalene or anthracene), respectively. Therefore, the contribution of the vibrational mode to the reorganization energy is divided into the contribution of the torsional mode and that of the π-bond stretching. The contribution of the π-bond stretching is subdivided again into thienothiophene and naphthalene (or anthracene). The reorganization energies originated from the vibrational frequencies less than 140 cm^{-1} in DH-TAT were smaller than those in the DH-TNT. This is due to the fact that the structure of the DH-TAT has heavier building blocks, and consequently, lower vibrational frequencies in the DH-TAT results in lower reorganization energy in that region. The contribution of the vibrational mode corresponding to the π-bond stretching of the thienothiophene in DH-TNT is larger than in the DH-TAT, while the contribution from the aromatic C=C bond in DH-TAT is larger than in the DH-TNT. The larger contribution from the thienothiophene in DH-TNT was also confirmed as the geometry changed

upon ionization to the cationic state as depicted at Figure 4: the root means square deviation (σ_{rms}) of bond lengths between two states were 0.018 Å and 0.012 Å for the DH-TNT and DH-TAT, respectively.

Next, the photoinduced dynamics of DH-TNT and DH-TAT were theoretically investigated with quantum chemical methods to study the excited state properties of DH-TNT and DH-TAT. In particlar, vertical absorption and fluorescence spectra were calculated and compared with the experimental data. For the excited properties of the vertical absorption related to the frontier orbital transition from HOMO to LUMO, the energy levels were investigated theoretically; furthermore, the energy levels of the HOMO and LUMO in the vertical absorption were compared with those in the vertical fluorescence.

With optimized geometries of the ground and excited states, the differences in the dihedral angle between the naphthalene (or anthracene) and the hexylthienothiophene were examined in the processes of photoinduced dynamics. For DH-TNT and DH-TAT, the dihedral angle of the optimized geometry for the ground state decreased from ~27° (for DH-TAT) or ~28° (for DH-TNT) to ~0° of the optimized geometry for the excited state. It is known that these changes of dihedral angles are a characteristic of an exciton self-trapping.[54-56] The similar dihedral angle in DH-TNT and DH-TAT shows that the steric hindrance between building blocks is almost the same.

Frontier molecular energy levels, first excitation energies (band gap), vertical absorption and fluorescence spectra of DH-TNT and DH-TAT are listed in Table 4. The calculated TD-DFT absorption spectra of DH-TNT and DH-TAT are

Table 4. The calculated vertical absorption (E$_A$, eV), fluorescence frequencies (E$_F$, eV) and their corresponding oscillator strengths (in the parenthesis) for DH-TNT and DH-TAT

		Method	DH-TNT	DH-TAT
$\varepsilon_{LUMO}-\varepsilon_{HOMO}$		Exptl.[a]	2.65	2.41
		DFT	3.42	2.98
		ZINDO	6.13 (3.20)	5.82 (3.09)
Ionization Potential	DFT	IP$_V$	6.17	6.00
		IP$_A$	5.99	5.86
Absorption	Exptl.[a]	E$_A$	3.26	2.83
	TD-DFT	E$_A$	3.11 (1.501)	2.69 (0.733)
		CI main coeff.	0.66 (H→L)	0.65 (H→L)
	ZINDO	E$_A$	2.90 (1.69)	2.81 (1.53)
		CI main coeff.	0.33 (H-1→L+1) 0.59 (H→L)	0.11 (H-2→L+2) -0.30 (H-1→L+1) 0.59 (H→L) -0.14 (H→L+2)
Fluorescence	Exptl.[a]	E$_F$	2.82	2.67
	TD-DFT (ES)	E$_F$	2.72 (1.95)	2.41 (1.14)

[a]Values from Ref. 33.

Theoretical Studies on Organic Semiconductor Materials

Bull. Korean Chem. Soc. **2012**, Vol. 33, No. 4   1217
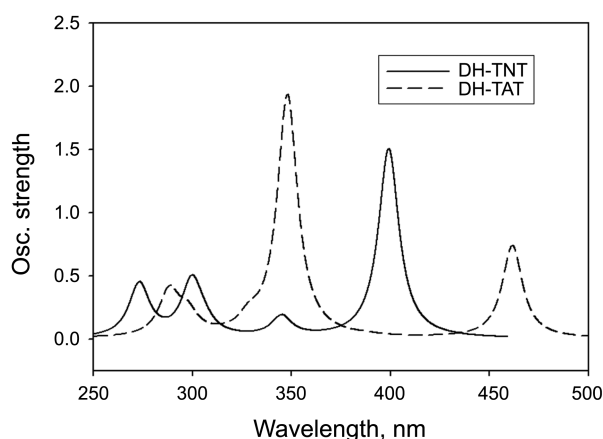
Figure 5. Calculated TD-DFT spectra of DH-TNT and DH-TAT.

Figure 6. Energy levels of frontier molecular orbitals of individual molecules.

Figure 7. HOMO (bottom) and LUMO (top) of DH-TAT. Hydrogen atoms are omitted for clarity.

displayed in Figure 5. All the theoretical results are well consistent with the experimental data in tendency. The calculated band gaps or energy gap between the LUMO and HOMO orbitals of DH-TNT and DH-TAT were qualitatively consistent with experimental results[33] i.e., 2.65 eV and 2.41 eV for DH-TNT and DH-TAT, respectively. The vertical ionization potentials of DH-TNT and DH-TAT obtained by B3LYP/6-31G(d,p) level were 6.17 eV and 6.00 eV, respectively, which are larger than that of pentacene (5.94 eV). These results confirm that DH-TNT and DH-TAT have good oxidative stability compared with that of pentacene. Comparing DH-TNT with DH-TAT, the hole mobility of the latter was higher than that of the former as the conjugation length of DH-TAT is longer than that of DH-TNT as reported by Kwon and coworkers.[33]

The absorption peaks of DH-TNT were estimated at 300 nm and 399 nm, and those of DH-TAT were estimated at 328 nm, 348 nm, and 462 nm using the TD-DFT method. On the other hand, experimental peaks appeared at 296 nm and 380 nm for DH-TNT, and 344 nm, 412 nm, and 438 nm for DH-TAT, respectively. Our theoretical results are well consistent with the experimental data,[33] considering that the experimental data were obtained in solution and the theoretical data were obtained in the gas phase.

Since the shapes of the frontier electronic level of individual monomers are strongly connected with the excited state properties of DH-TNT and DH-TAT,[57] the orbital energies of the HOMO and LUMO of the individual monomer and two organic semiconductor materials were investigated in the process of the vertical absorption. This approach is useful,[58] because the S_1 state is indeed mainly composed of a HOMO-LUMO transition, and the major coefficients of configuration interaction (CI) are obtained by the orbital transition from HOMO to LUMO. The energy levels of the frontier molecular orbitals of fragment molecules and two semiconductor materials are shown in Figure 6.

The HOMO energy level of hexyl thienothiophene (HTT) is located well between the HOMOs of naphthalene and anthracene, while the LUMO level of HTT was much higher than those of naphthalene or anthracene. Therefore, the electron density o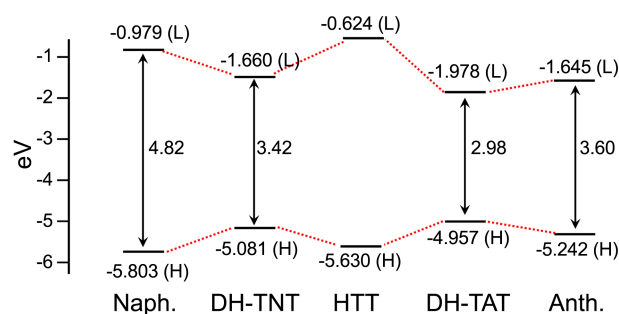f HOMO is well distributed in both the thienothiophene moiety of HTT and acene units: however, electron density of LUMO is localized at the acene moiety as shown at Figure 7.
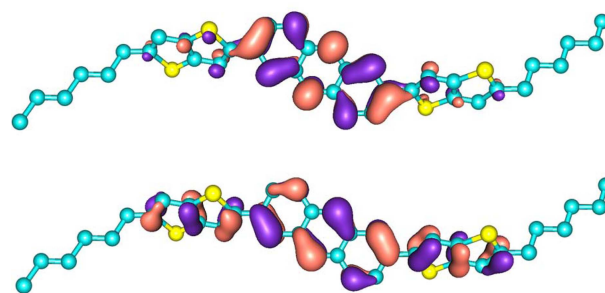
The calculated HOMO-LUMO energy gaps of DH-TNT and DH-TAT in the vertical absorption with TD-DFT were 3.42 eV and 2.98 eV, respectively, which are much smaller than those with the ZINDO method: 6.13eV and 5.82 eV, respectively. As summarized by Sun *et al.*,[56,59] an electron and a hole are in the range of the attractive potential in the ZINDO method and an effective electron-hole attraction stabilizes the HOMO-LUMO gap. In general, an electron and a hole are in the range of the repulsive potential in the TD-DFT/DFT method, which decreases the band gap of conjugated polymers. Nevertheless, the values estimated by TD-DFT are much closer to the experimental values.

Figure 8 shows the HOMO-LUMO energy gaps of DH-TNT and DH-TAT in the vertical absorption and the vertical fluorescence process. The calculated HOMO-LUMO energy gap of DH-TNT in the vertical absorption was larger than
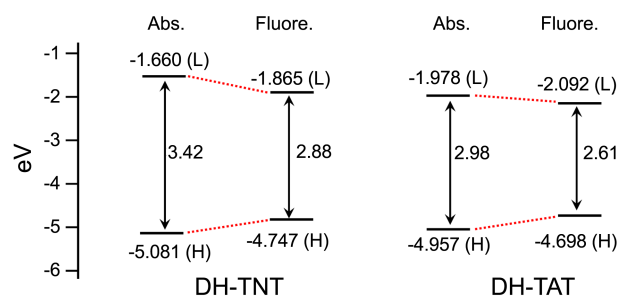

Figure 8. Energy levels of frontier molecular orbitals in the vertical absorption and in the vertical fluorescence.

that in the vertical fluorescence by 0.54 eV, while the energy gap difference was 0.37 eV in the DH-TAT.

The lower gap difference of HOMO-LUMO for DH-TAT implies more effective π-conjugation.[56,60] These theoretical results were also supported experimentally by the fact that the mobility of DH-TAT is superior to that of DH-TNT as reported by Kwon and coworkers.[33]

Conclusions

The TFT characteristics and the excited state properties of 2,6-bis(5'-hexyl-thieno[3,2-*b*]thiophene-2'-yl)naphthalene (DH-TNT) and 2,6-bis(5'-hexyl-thieno[3,2-*b*]thiophene-2'-yl)anthracene (DH-TAT) were calculated and the results were compared with experimental values. The theoretical results on the OTFT properties of DH-TNT and DH-TAT as organic semiconductor materials were consistent with the experimental results.

The main contribution of hole transfer to the reorganization energy is attributed to the torsional distortion along the C-C bond between the thienothiophene group and acene moiety, and the reorganization energy caused by the vibrational distortion at the DH-TNT was larger than that of DH-TAT because of the lighter building block of DH-TNT.

According to the results of the spectroscopic property of the DH series, the absorption peaks of DH-TNT and DH-TAT were well consistent with the experimental data, considering that the experimental data were obtained in solution and the theoretical data were obtained in a gas phase. In addition, the energies and densities of frontier orbital HOMOs and LUMOs of the building blocks showed that the interaction between the building blocks in DH-TAT is larger than that in DH-TNT, and thus π-conjugation in DH-TAT is more effective than that in DH-TNT.

References

1. Garnier, F.; Hajlaoui, R.; Yassar, A.; Srivastava, P. *Science* **1994**, *265*, 1684.
2. Horowitz, G.; Fichou, D.; Peng, X. Z.; Xu, Z. G.; Garnier, F. *Solid State Commun.* **1989**, *72*, 381.
3. Horowitz, G. *Adv. Mater.* **1998**, *10*, 365.
4. Sirringhaus, H.; Brown, P. J.; Friend, R. H.; Nielsen, M. M. K.; Langeveld-Voss, B. M. W.; Spiering, A. J. H.; Janssen, A. J.; Meijer, E. W.; Herwig, P.; De Leeuw, D. M. *Nature (London)* **1999**, *401*, 685.
5. Katz, H. E.; Lovinger, A. J.; Johnson, J.; Kloc, C.; Siegrist, T.; Li, W.; Lin, Y. Y.; Dodabalapur, A. *Nature (London)* **2000**, *404*, 478.
6. Tang, C. W.; VanSlyke, S. A. *Appl. Phys. Lett.* **1987**, *51*, 913.
7. Burroughes, J. H.; Bradley, D. D. C.; Brown, A. R.; Marks, R. N.; Mackay, K.; Friend, R. H.; Burns, P. L.; Holmes, A. B. *Nature*

(London) **1990**, *347*, 539.
8. Sheats, J. R.; Antoniadis, H.; Hueschen, M.; Leonard, W.; Miller, J. R.; Roitman, D.; Stocking, A. *Science* **1996**, *273*, 884.
9. Friend, R. H.; Gymer, R. W.; Holmes, A. B.; Burroughes, J. H.; Marks, R. N.; Taliani, C.; Bradley, D. D. C.; Dos Santos, D. A.; Brédas, J. L.; Logdlund, M.; Salaneck, W. R. *Nature (London)* **1999**, *397*, 121.
10. Sariciftci, N. S.; Smilowitz, L.; Heeger, A. J.; Wudl, F. *Science* **1992**, *258*, 1474.
11. Halls, J. J. M.; Walsh, C. A.; Greenham, N. C.; Marseglia, E. A.; R. H.; Moratti, S. C.; Holmes, A. B. *Nature (London)* **1995**, *376*, 498.
12. Yu, G.; Wang, J.; McElvain, J.; Heeger, A. *J. Adv. Mater.* **1998**, *10*, 1431.
13. Brabec, C. J.; Sariciftci, N. S.; Hummelen, J. C. *Adv. Funct. Mater.* **2001**, *11*, 15.
14. Katz, H. E. *J. Mater. Chem.* **1997**, *7*, 369.
15. Nelson, S. F.; Lin, Y. Y.; Gundlach, D. J.; Jackson, T. N. *Appl. Phys. Lett.* **1998**, *72*, 1854.
16. Klauk, H.; Gundlach, D. J.; Bonses, M.; Kuo, C. C.; Jackson, T. N. *Appl. Phys. Lett.* **2000**, *76*, 1692.
17. Kelley, T. W.; Muyres, D. V.; Baude, P. F.; Smith, T. P.; Jones, T. D. *Mater. Res. Soc. Symp. Proc.* **2003**, *771*, 169.
18. Halik, M.; Klank, H.; Zschieschang, U.; Schmid, G.; Ponomarenko, S.; Kirchmeyer, S.; Weber, W. *Adv. Mater.* **2003**, *15*, 917.
19. Katz, H. E.; Dodabalapur, A.; Torsi, L.; Elder, D. *Chem. Mater.* **1995**, *7*, 2238.
20. Sirrinhaus, H.; Friend, R. H.; Li, X. C.; Moratti, S. C.; Holmes, A. B.; Feeder, N. *Appl. Phys. Lett.* **1997**, *71*, 3871.
21. Ito, K.; Suzuki, T.; Sakamoto, Y.; Kubota, D.; Inoue, Y.; Sato, F.; Tokito, S. *Angew. Chem.* **2003**, *115*, 1191.
22. Afzali, A.; Dimitrakopoulos, C. D.; Breen, T. C. *J. Am. Chem. Soc.* **2002**, *124*, 8812.
23. Bao, Z.; Lovinger, A. J.; Dodabalapur, A. *Appl. Phys. Lett.* **1996**, *69*, 3066.
24. Tang, Q.; Li, H.; He, M.; Hu, W.; Liu, C.; Chen, K.; Wang, C.; Liu, Y.; Zhu, D. *Adv. Mater.* **2006**, *18*, 65.
25. Ong, B. S.; Wu, Y.; Liu, P.; Gardner, S. *J. Am. Chem. Soc.* **2004**, *126*, 3378.
26. Fuchigami, H.; Tsumura, A.; Koezuka, H. *Appl. Phys. Lett.* **1993**, *63*, 1372.
27. Newman, C. R.; Frisbie, C. D.; da Silva Filho, D. A.; Bredas, J.-L.; Ewbank, P. C.; Mann, K. R. *Chem. Mater* **2004**, *16*, 4436.
28. Katz, H. E.; Bao, Z.; Gilat, S. L. *Acc. Chem. Res.* **2001**, *34*, 359.
29. Facchetti, A.; Mushrush, M.; Katz, H. E.; Marks, T. J. *Adv. Mater.* **2003**, *15*, 33.
30. Hong, X. M.; Katz, H. E.; Lovinger, A. J.; Wang, B.-C.; Raghavachari, K. *Chem. Mater.* **2001**, *13*, 4686.
31. Carnier, F.; Yassar, A.; Hajlaoui, R.; Horowitz, G.; Deloffre, F.; Servet, B.; Ries, S.; Alnot, P. *J. Am. Chem. Soc.* **1993**, *115*, 8716.
32. Dimitrakopoulos, C. D.; Furman, B. K.; Graham, T.; Hedge, S.; Purushothaman, S. *Synth. Met.* **1998**, *92*, 47.
33. Kim, H. S.; Kim, Y, H,; Kim, T. H.; Noh, Y. Y.; Pyo, S.; Yi, M. H.; Kim, D. Y.; Kwon, S. K. *Chem. Mater.* **2007**, *19*, 3561.
34. Merlo, J. A.; Newman, C. R.; Gerlach, C.; Kelly, T. W.; Muyres, D. V.; Fritz, S. E.; Toney, M. F.; Frisbie, C. D. *J. Am, Chem. Soc.* **2005**, *127*, 3997.
35. Meng, H.; Sun, F.; Goldfinger, M. B.; Jaycox, G. D.; Li, Z.; Marshall, W. J.; Blackman, G. S. *J. Am. Chem. Soc.* **2005**, *127*, 2406.
36. Lim, E.; Jung, B. J.; Shim, H. K. *Macromol.* **2003**, *36*, 4228.
37. Lim, E.; Jung. B. J.; Lee, J.; Shim, H. K.; Lee, J. I.; Yang, Y. S.; Do, L. M. *Macromol.* **2005**, *38*, 4531.
38. Noh, Y. Y.; Azumi, R.; Goto, M.; Jung, B. J.; Lim, E.; Shim, H. K.; Yoshida, Y.; Yase, K.; Kim, D. Y. *Chem. Mater.* **2005**, *17*, 3861.
39. Brédas, J. L.; Beljonne, D.; Coropceanu, V.; Cornil, J. *Chem. Rev.* **2004**, *104*, 4971 and references cited therein.

40. Marcus, R. A. *Rev. Mod. Phys.* **1993**, *65*, 599.
41. (a) Brédas, J.-L.; Calbert, J. P.; da Silva Filho, D. A.; Cornil, J. *Proc. Natl. Acad. Sci. USA* **2002**, *99*, 5804. (b) Park, Y. H.; Yang, K.; Kim, Y.-H.; Kwon, S. K. *Bull. Korean Chem. Soc.* **2007**, *28*, 1358.
42. Balzani, V., Ed., *Electron Transfer in Chemistry*; Wiley-VCH: Weinheim, 2001.
43. (a) Bixon, M., Jortner, J., Eds.; Electron Transfer: From Isolated Molecules to Biomolecules, *Adv. Chem. Phys.* Wiley: New York, **1999**; Vols. 106-107. (b) Marcus, R. A. *J. Chem. Phys.* **1956**, *24*, 966 and 979. (c) Marcus, R. A.; Sutin, N. *Biochim. Biophys. Acta* **1985**, *811*, 265.
44. Reimers, J. R. *J. Chem. Phys.* **2001**, *115*, 9103.
45. Silinsh, E. A.; Klimkans, A.; Larsson, S.; Capek, V. *Chem. Phys.* **1995**, *198*, 31.
46. Frisch, M. J.; Trucks, G. W.; Schlegel, H. B.; Scuseria, G. E.; Robb, M. A.; Cheeseman, J. R.; Zakrzewski, V. G.; Montgomery, J. A., Jr.; Stratmann, R. E.; Burant, J. C.; Dapprich, S.; Millam, J. M.; Daniels, A. D.; Kudin, K. N.; Strain, M. C.; Farkas, O.; Tomasi, J.; Barone, V.; Cossi, M.; Cammi, R.; Mennucci, B.; Pomelli, C.; Adame, C.; Clifford, S.; Ochterski, J.; Petersson, G. A.; Ayala, P. Y.; Cui, Q.; Morokuma, K.; Salvador, P.; Dannenberg, J. J.; Malick, D. K.; Rabuck, A. D.; Raghavachari, K.; Foresman, J. B.; Cioslowski, J.; Ortiz, J. V.; Baboul, A. G.; Stefanov, B. B.; Liu, G.; Liashenko, A.; Piskorz, P.; Komaromi, I.; Gomperts, R.; Martin, R. L.; Fox, D. J.; Keith, T.; Al-Laham, M. A.; Peng, C. Y.; Nanayakkara, A.; Challacombe, M.; Gill, P. M.W.; Johnson, B.; Chen, W.; Wong, M. W.; Andres, J. L.; Gonzalez, C.; HeadGordon, M.; Replogle, E. S.; Pople, J. A. *Gaussian 98*, Revision A.7: Gaussian, Inc., Pittsburgh, PA, 1998.
47. Frisch, M. J. *et al. Gaussian 03*, Revision B. 05, Gaussian, Inc., Pittsburgh, PA, 2003.
48. (a) Becke, A. D. *J. Chem. Phys.* **1993**, *98*, 5648. (b) Lee, C.; Yang, W.; Parr, R. G. *Phys. Rev. B* **1988**, *37*, 785.
49. Stratmann, R. E.; Scuseria, G. E.; Frisch, M. J. *J. Chem. Phys.* **1998**, *109*, 8218.
50. (a) Zerner, M. C.; Correa de Mello, P.; Hehenberger, M. *Int. J. Quant. Chem.* **1982**, *21*, 251. (b) Hanson, L. K.; Fajer, J.; Thompson, M. A.; Zerner, M. C. *J. Am. Chem. Soc.* **1987**, *109*, 4728.
51. Thompson, M. A.; Xerner, M. C. *J. Am. Chem. Soc.* **1991**, *113*, 8210.
52. Foresman, J. B.; Head-Corden, M.; Pople, J. A.; Frisch, M. J. *J. Phys. Chem.* **1992**, *96*, 135.
53. Sancho-Garcia, J. C.; Poulsen, J.; Gierschner, J.; Martinez-Alvárez, R.; Hennebicq, E.; Hanack, M.; Egelhaaf, H. J.; Oelkrug, D.; Beljonne, D.; Brédas, J. L.; Cornil, *J. Adv. Mater.* **2004**, *16*, 1193.
54. Hennebicq, E.; Pourtois, G.; Scholes, G. D.; Herz, L. M.; Russell, D. M.; Silva, C.; Setayesh, S.; Grimsdale, A. C.; Müellen, K.; Brédas, J. L.; Beljonne, D. *J. Am. Chem. Soc.* **2005**, *127*, 4744.
55. Brédas, J. L.; Cornil, J.; Beljonne, D.; dos Santos, D. A.; Shuai, Z. *Acc. Chem. Res.* **1999**, *32*, 267.
56. Sun, M. T. *Chem. Phys.* **2006**, *320*, 155.
57. Cornil, J.; Gueli, I.; Dkhissi, A.; Sancho-Garcia, J. C.; Hennebicq, E.; Calbert, J. P.; Lemaur, V.; Beljonne, D.; Brédas, J. L. *J. Chem. Phys.* **2003**, *118*, 6615.
58. Tretiak, S.; Igumenshchev, K.; Chernyak, V. *Phys. Rev. B* **2005**, *71*, 033201.
59. (a) Sun, M. T.; Pullerits, T.; Kjellberg, P.; Pullerits, W. J. D.; Han, K. L. *J. Phys. Chem. A* **2006**, *110*, 6324. (b) Sun, M. T. *J. Chem. Phys.* **2006**, *124*, 054903. (c) Sun, M. T.; Ma, F. C. *J. Theoret. Comput. Chem.* **2006**, *5*, 163.
60. Ando, S.; Nishida, J. I.; Fujiwara, E.; Tada, H.; Inoue, Y.; Tokito, S.; Yamashita, Y. *Chem. Mater.* **2005**, *17*, 1261.